Is the Molecular Berry Phase an Artifact of the Born-Oppenheimer Approximation?

Seung Kyu Min,[1,2] Ali Abedi,[1,3] Kwang S. Kim,[2] and E. K. U. Gross[1,3]

[1]*Max-Planck Institut für Mikrostrukturphysik, Weinberg 2, D-06120 Halle, Germany*
[2]*Department of Chemistry, School of Natural Science, Ulsan National Institute of Science and Technology (UNIST),
Ulsan 689-798, Korea*
[3]*European Theoretical Spectroscopy Facility (ETSF)*

We demonstrate that the molecular Berry phase and the corresponding nonanalyticity in the electronic Born-Oppenheimer wave function is, in general, not a true topological feature of the exact solution of the full electron-nuclear Schrödinger equation. For a numerically exactly solvable model we show that a nonanalyticity, and the associated geometric phase, only appear in the limit of infinite nuclear mass, while a perfectly smooth behavior is found for any finite nuclear mass.

Geometric phases are ubiquitous in physics and chemistry, and some of the most fascinating phenomena in condensed matter science such as topological insulators [1,2], ferroelectrics [3,4], the Aharonov-Bohm effect [5], as well as conical intersections in molecules [6–10] are closely associated with Berry phases. Geometric phases may arise when the Hamiltonian of a system depends on a set of parameters $\underline{\mathbf{R}}$. In Berry's original definition [11], this parameter set is allowed to change adiabatically, i.e., very slowly in time along a given path $C = \{\underline{\mathbf{R}}(t')|t' \in [t_0, t]\}$, such that the solution of the time-dependent Schrödinger equation,

$$i\frac{\partial}{\partial t}\Phi_n(\underline{\mathbf{r}}; t) = \hat{H}^{\mathrm{BO}}(\underline{\mathbf{r}}; \underline{\mathbf{R}}(t))\Phi_n(\underline{\mathbf{r}}; t), \qquad (1)$$

by virtue of the adiabatic theorem, is given by

$$\Phi_n(\underline{\mathbf{r}}; t) = e^{-i\int_{t_0}^{t} \epsilon_n^{\mathrm{BO}}(\underline{\mathbf{R}}(t'))dt'} e^{-i\gamma_n(C)}\Phi_n^{\mathrm{BO}}(\underline{\mathbf{r}}; \underline{\mathbf{R}}(t)), \qquad (2)$$

where

$$\hat{H}^{\mathrm{BO}}(\underline{\mathbf{r}}; \underline{\mathbf{R}})\Phi_n^{\mathrm{BO}}(\underline{\mathbf{r}}; \underline{\mathbf{R}}) = \epsilon_n^{\mathrm{BO}}(\underline{\mathbf{R}})\Phi_n^{\mathrm{BO}}(\underline{\mathbf{r}}; \underline{\mathbf{R}}). \qquad (3)$$

In Eq. (2), the first exponent is a dynamical phase which appears naturally from the time-dependent Schrödinger equation while the second exponent, $\gamma_n(C)$, is given in terms of the Berry connection,

$$\mathbf{A}_{\nu,n}^{\mathrm{BO}}(\underline{\mathbf{R}}) = \langle\Phi_n^{\mathrm{BO}}(\underline{\mathbf{R}})| - i\nabla_\nu\Phi_n^{\mathrm{BO}}(\underline{\mathbf{R}})\rangle_{\underline{\mathbf{r}}}, \qquad (4)$$

as a line integral along the path C

$$\begin{aligned}\gamma_n^{\mathrm{BO}}(C) &= \int_C \sum_\nu \mathbf{A}_{\nu,n}^{\mathrm{BO}}(\underline{\mathbf{R}}) \cdot d\mathbf{R}_\nu \\ &= \sum_\nu \int_{t_0}^{t} dt' \mathbf{A}_{\nu,n}^{\mathrm{BO}}(\underline{\mathbf{R}}(t')) \cdot \frac{d\mathbf{R}_\nu(t')}{dt'}. \end{aligned} \qquad (5)$$

The notation $\langle\cdots\rangle_{\underline{\mathbf{r}}}$ indicates integration over $\underline{\mathbf{r}}$-space only. All quantities in this Letter are in atomic units (a.u.), and a bold value with underline represents a multidimensional vector, i.e., $\underline{\mathbf{X}} \equiv \{\mathbf{X}_\nu|\nu = 1, \cdots\}$. When C becomes a closed loop $\mathcal{L}$ this line integral,

$$\gamma_n^{\mathrm{BO}}(\mathcal{L}) = \oint_{\mathcal{L}} \sum_\nu \mathbf{A}_{\nu,n}^{\mathrm{BO}}(\underline{\mathbf{R}}) \cdot d\underline{\mathbf{R}}_\nu, \qquad (6)$$

may give a nonvanishing value if the loop encloses a conical intersection (CI). The value of $\gamma_n^{\mathrm{BO}}(\mathcal{L})$ does not depend on the shape of $\mathcal{L}$ as long as the loop encloses the CI. While the concept displayed in Eqs. (1)–(6) is completely general, i.e., may refer to any Hamiltonian that depends on a set of parameters $\underline{\mathbf{R}}$, the specific case the notation in Eqs. (1)–(6) refers to is the molecular Berry phase appearing in the Born-Oppenheimer (BO) approximation. The latter is fundamental to all modern condensed matter theory. It derives from the fact that, in most cases, the nuclei move extremely slowly compared to the electrons. Hence, as a first step, it is reasonable to neglect the nuclear kinetic energy operator in the complete molecular Hamiltonian leading to the so-called BO Hamiltonian,

$$\hat{H}^{\mathrm{BO}}(\underline{\mathbf{r}}; \underline{\mathbf{R}}) = \hat{T}_e(\underline{\mathbf{r}}) + \hat{V}_{ee}(\underline{\mathbf{r}}) + \hat{V}_{en}(\underline{\mathbf{r}}, \underline{\mathbf{R}}) + \hat{V}_{nn}(\underline{\mathbf{R}}). \quad (7)$$

Here, $\hat{T}_e$ is the electronic kinetic energy operator, $\hat{V}_{ee}(\hat{V}_{nn})$ is the repulsive electron-electron (nuclear-nuclear) interaction, and $\hat{V}_{en}$ is the electron-nuclear Coulomb attraction. The complete molecular wave function can then be approximated by the adiabatic ansatz $\Psi_{\mathrm{mol}}^{\mathrm{BO}}(\underline{\mathbf{r}}, \underline{\mathbf{R}}) = \chi_{kn}^{\mathrm{BO}}(\underline{\mathbf{R}})\Phi_n^{\mathrm{BO}}(\underline{\mathbf{r}}; \underline{\mathbf{R}})$, where $\chi_{kn}^{\mathrm{BO}}(\underline{\mathbf{R}})$ satisfies the Schrödinger equation

$$\left[\sum_\nu \frac{(-i\nabla_\nu + \mathbf{A}_{\nu,n}^{\mathrm{BO}})^2}{2M_\nu} + \tilde{\epsilon}_n^{\mathrm{BO}}(\underline{\mathbf{R}})\right]\chi_{kn}^{\mathrm{BO}}(\underline{\mathbf{R}}) = E_{kn}\chi_{kn}^{\mathrm{BO}}(\underline{\mathbf{R}}), \qquad (8)$$

263004-1

with the generalized BO potential energy surface

$$\tilde{\epsilon}_n^{\mathrm{BO}}(\underline{\mathbf{R}}) = \langle \Phi_n^{\mathrm{BO}}(\underline{\mathbf{R}})|\hat{H}_{\mathrm{BO}}(\underline{\mathbf{R}})|\Phi_n^{\mathrm{BO}}(\underline{\mathbf{R}})\rangle_{\mathbf{r}}$$
$$+ \sum_\nu \frac{\langle \nabla_\nu \Phi_n^{\mathrm{BO}}(\underline{\mathbf{R}})|\nabla_\nu \Phi_n^{\mathrm{BO}}(\underline{\mathbf{R}})\rangle_{\mathbf{r}}}{2M_\nu} - \sum_\nu \frac{\mathbf{A}_{\nu,n}^{\mathrm{BO}}(\underline{\mathbf{R}})^2}{2M_\nu}.$$

(9)

Here, M_ν is the mass of the νth nucleus. After the seminal work of Mead and Truhlar [12], a lot of attention has been devoted to the molecular Berry phase associated with the vector potential, Eq. (4) [13,14]. An essential aspect of the molecular geometric phase is that it always appears in the presence of some kind of nonanalyticity in the $\underline{\mathbf{R}}$-dependence of $\epsilon_n^{\mathrm{BO}}(\underline{\mathbf{R}})$ and $\Phi_n^{\mathrm{BO}}(\mathbf{r}; \underline{\mathbf{R}})$. Similar to Cauchy's theorem in complex analysis, where a loop integral in the complex plane picks up a phase if the loop encloses a pole, the line integral in Eq. (6) may pick up a Berry phase if the loop encloses a CI of BO surfaces. Clearly, in the case of the molecular Berry phase, the parametric dependence of the Hamiltonian in Eq. (3) is the result of an approximation, the BO approximation. In the full molecular Hamiltonian, $\underline{\mathbf{R}}$ is a dynamical variable. The objective of this Letter is to investigate whether this very specific topological feature, this nonanalyticity in the $\underline{\mathbf{R}}$-dependence of the wave function,

only occurs within the BO approximation or whether it may survive as a feature of the full molecular wave function $\Psi_{\mathrm{mol}}(\mathbf{r}, \underline{\mathbf{R}})$, i.e., as a true feature of nature. To investigate this question, we employ the recently derived framework of exact factorization of $\Psi_{\mathrm{mol}}(\mathbf{r}, \underline{\mathbf{R}})$ [15–19]. This formulation lends itself as a natural framework because it leads to a Berry-type vector potential but without invoking the BO approximation.

Within this formulation, $\Psi_{\mathrm{mol}}^N(\mathbf{r}, \underline{\mathbf{R}})$, the exact Nth eigenstate of the full molecular Schrödinger equation $\hat{H}(\mathbf{r}, \underline{\mathbf{R}})\Psi_{\mathrm{mol}}^N(\mathbf{r}, \underline{\mathbf{R}}) = E_N \Psi_{\mathrm{mol}}^N(\mathbf{r}, \underline{\mathbf{R}})$, can be factorized as a single product $\Psi_{\mathrm{mol}}^N(\mathbf{r}, \underline{\mathbf{R}}) = \chi_N(\underline{\mathbf{R}})\Phi_N(\mathbf{r}; \underline{\mathbf{R}})$, where $\Phi_N(\mathbf{r}; \underline{\mathbf{R}})$ satisfies the partial normalization condition, $\int d\mathbf{r}|\Phi_N(\mathbf{r}; \underline{\mathbf{R}})|^2 = 1$. The equations which $\Phi_N(\mathbf{r}; \underline{\mathbf{R}})$ and $\chi_N(\underline{\mathbf{R}})$ satisfy are

$$[\hat{H}^{\mathrm{BO}}(\mathbf{r}; \underline{\mathbf{R}}) + \hat{U}_{en}(\mathbf{r}, \underline{\mathbf{R}})]\Phi_N(\mathbf{r}; \underline{\mathbf{R}}) = \epsilon_N^{\mathrm{ex}}(\underline{\mathbf{R}})\Phi_N(\mathbf{r}; \underline{\mathbf{R}}),$$

(10)

$$\left[\sum_\nu \frac{(-i\nabla_\nu + \mathbf{A}_{\nu,N}^{\mathrm{ex}})^2}{2M_\nu} + \epsilon_N^{\mathrm{ex}}(\underline{\mathbf{R}})\right]\chi_N(\underline{\mathbf{R}}) = E_N \chi_N(\underline{\mathbf{R}}),$$

(11)

where $\hat{U}_{en}$ is an electron-nucleus coupling operator given by

$$\hat{U}_{en}(\mathbf{r}, \underline{\mathbf{R}}) = \sum_\nu \frac{1}{M_\nu}\left[\frac{(-i\nabla_\nu - \mathbf{A}_{\nu,N}^{\mathrm{ex}})^2}{2} + \left(\frac{-i\nabla_\nu \chi_N}{\chi_N} + \mathbf{A}_{\nu,N}^{\mathrm{ex}}\right) \cdot (-i\nabla_\nu - \mathbf{A}_{\nu,N}^{\mathrm{ex}})\right].$$

(12)

$\epsilon_N^{\mathrm{ex}}(\underline{\mathbf{R}})$ is defined as

$$\epsilon_N^{\mathrm{ex}}(\underline{\mathbf{R}}) = \langle \Phi_N(\underline{\mathbf{R}})|\hat{H}_{\mathrm{BO}}(\underline{\mathbf{R}})|\Phi_N(\underline{\mathbf{R}})\rangle_{\mathbf{r}}$$
$$+ \sum_\nu \frac{\langle \nabla_\nu \Phi_N(\underline{\mathbf{R}})|\nabla_\nu \Phi_N(\underline{\mathbf{R}})\rangle_{\mathbf{r}}}{2M_\nu} - \sum_\nu \frac{\mathbf{A}_{\nu,N}^{\mathrm{ex}}(\underline{\mathbf{R}})^2}{2M_\nu},$$

(13)

and

$$\mathbf{A}_{\nu,N}^{\mathrm{ex}}(\underline{\mathbf{R}}) = \langle \Phi_N(\underline{\mathbf{R}})| - i\nabla_\nu \Phi_N(\underline{\mathbf{R}})\rangle_{\mathbf{r}}.$$

(14)

Because $\epsilon_N^{\mathrm{ex}}(\underline{\mathbf{R}})$ and $\mathbf{A}_N^{\mathrm{ex}}(\underline{\mathbf{R}})$ yield the exact many-body nuclear density, $|\chi_N(\underline{\mathbf{R}})|^2 = \int d\mathbf{r}|\Psi_{\mathrm{mol}}^N(\mathbf{r}, \underline{\mathbf{R}})|^2$, and the exact many-body nuclear current density, $1/M_\nu(\mathrm{Im}[\chi_N^* \nabla_\nu \chi_N] + |\chi_N|^2 \mathbf{A}_{\nu,N}^{\mathrm{ex}}) = 1/M_\nu(\mathrm{Im}\int d\mathbf{r}\Psi_{\mathrm{mol}}^{N*}\nabla_\nu \Psi_{\mathrm{mol}}^N)$, we can call $\epsilon_N^{\mathrm{ex}}(\underline{\mathbf{R}})$ and $\mathbf{A}_N^{\mathrm{ex}}(\underline{\mathbf{R}})$ the exact scalar potential and the exact vector potential. They are unique up to gauge transformations, $\chi_N(\underline{\mathbf{R}}) \to \chi_N(\underline{\mathbf{R}})e^{iS(\underline{\mathbf{R}})}$ and $\Phi_N(\underline{\mathbf{R}}) \to \Phi_N(\underline{\mathbf{R}})e^{-iS(\underline{\mathbf{R}})}$ [17,18].

Both the exact molecular wave function $\Psi_{\mathrm{mol}}^N(\mathbf{r}, \underline{\mathbf{R}}) = \chi_N(\underline{\mathbf{R}})\Phi_N(\mathbf{r}; \underline{\mathbf{R}})$ and the adiabatic approximation $\Psi_{\mathrm{mol}}^{\mathrm{BO}}(\mathbf{r}, \underline{\mathbf{R}}) = \chi_{kn}^{\mathrm{BO}}(\underline{\mathbf{R}})\Phi_n^{\mathrm{BO}}(\mathbf{r}; \underline{\mathbf{R}})$ are given in terms of a single product of a nuclear and an electronic wave function where the latter satisfies the partial normalization condition

$\int |\Phi(\mathbf{r}; \underline{\mathbf{R}})|^2 d\mathbf{r} = 1$ for each nuclear configuration $\underline{\mathbf{R}}$. Both in the exact case and in the adiabatic approximation, the nuclear factor satisfies a standard Schrödinger equation [Eqs. (11) and (8), respectively] with a vector potential [Eqs. (14) and (4), respectively] and a scalar potential [Eqs. (13) and (9), respectively] that formally follow the same expression. In particular, the vector potential is defined as a Berry connection in both cases. The only difference is that in the adiabatic approximation the Berry connection $\underline{\mathbf{A}}_n^{BO}(\underline{\mathbf{R}})$, Eq. (4), and the BO potential energy surfaces $\tilde{\epsilon}_n^{\mathrm{BO}}(\underline{\mathbf{R}})$, Eq. (9), are evaluated from the BO electronic wave function $\Phi_n^{\mathrm{BO}}(\mathbf{r}; \underline{\mathbf{R}})$ while the exact Berry connection $\underline{\mathbf{A}}_N^{\mathrm{ex}}(\underline{\mathbf{R}})$, Eq. (14), and the exact potential energy surfaces $\epsilon_N^{\mathrm{ex}}(\underline{\mathbf{R}})$, Eq. (13), are evaluated with the exact electronic wave function coming from Eq. (10). In this sense $\underline{\mathbf{A}}_N^{\mathrm{ex}}(\underline{\mathbf{R}})$ represents a feature of the exact molecular wave function. Can this "exact Berry connection" have the fascinating topological structure that gives rise to a non-vanishing Berry phase?

This is the question we are going to address in the following by studying a two-dimensional model system which, in the BO approximation, has CIs leading to a Berry phase, and which, at the same time, is simple enough to allow for a numerically exact solution.

The system is a 2D generalization of a model proposes by Shin and Metiu [20]. It consists of three ions and an electron. Two of the ions are fixed at $(\pm L/2, 0)$, and the third ion as well as the electron are allowed to move in two-dimensional space. Representing the positions of the moving ion and the electron as $\mathbf{R} = (X, Y)$ and $\mathbf{r} = (x, y)$, respectively, the full Hamiltonian is

$$\hat{H}(\mathbf{r}, \mathbf{R}) = -\frac{1}{2M}\nabla_{\mathbf{R}}^2 - \frac{1}{2}\nabla_{\mathbf{r}}^2 + V_{en}\left(\left|\mathbf{r} - \left(\frac{L}{2}, 0\right)\right|\right)$$

$$+ V_{en}\left(\left|\mathbf{r} - \left(-\frac{L}{2}, 0\right)\right|\right) + V_{en}(|\mathbf{r} - \mathbf{R}|)$$

$$+ V_{nn}\left(\left|\mathbf{R} - \left(\frac{L}{2}, 0\right)\right|\right) + V_{nn}\left(\left|\mathbf{R} - \left(-\frac{L}{2}, 0\right)\right|\right)$$

$$+ V_{nn}(L) + (R/R_0)^4, \tag{15}$$

where the first two terms are the kinetic energy operators for the moving ion and the electron, respectively, and the electron-nucleus interaction potential, $V_{en}(x) = -1/\sqrt{a + x^2}$, and the nucleus-nucleus interaction potential, $W_{nn}(x) = 1/\sqrt{b + x^2}$, are represented as soft Coulomb potentials while the last term is added to make the system bound. Here, the origin is set as the center of the two fixed ions. We choose parameters a, b, R_0, and L as 0.5, 10.0, 3.5, and $4\sqrt{3}/5$, respectively. Since the interaction potentials for the three ions are identical, we can expect that symmetry-induced degenerate states exist at equilateral positions $\mathbf{R}_{eq}^{\pm} = (0, \pm Y_{eq})$, where $Y_{eq} = \sqrt{3}/2L = 1.2$ with D_{3h} point group symmetry.

In Fig. 1, we present the first and second excited BO surfaces, $\epsilon_1^{BO}(\mathbf{R})$ and $\epsilon_2^{BO}(\mathbf{R})$, respectively, with the corresponding real-valued BO electronic wave functions $\Phi_{1,2}^{BO}(\mathbf{r}; \mathbf{R})$, which are numerical eigenstates of the BO Hamiltonian [21]. Indeed, we can confirm the degeneracy between the energy levels ϵ_1^{BO} and ϵ_2^{BO} at $\mathbf{R}_{eq}^{\pm}$ where the energy is -0.286. (Since the s-orbital-like ground BO electronic state is not related to CIs, we focus only on $\Phi_{1,2}^{BO}$.) To visualize possible nonanalyticities in the wave function $\Phi_{1,2}^{BO}(\mathbf{r}; \mathbf{R})$ with respect to $\mathbf{R}$, we investigate the two-dimensional vector field $\int \mathbf{r}\Phi(\mathbf{r}; \mathbf{R})d\mathbf{r}$ whose direction in space represents the "polarization of the wave function": A p-orbital-like electronic wave function, $\Phi(\mathbf{r}; \mathbf{R})$, can be represented as a vector pointing from the region of negative values of $\Phi(\mathbf{r}; \mathbf{R})$ to the region of positive values of $\Phi(\mathbf{r}; \mathbf{R})$ in $\mathbf{r}$-space as depicted in Fig. 1(b). The discontinuities of $\Phi(\mathbf{r}; \mathbf{R})$ appearing in $\mathbf{R}$-space can then be seen as abrupt changes in the direction of the vectors. We find that a discontinuous phase change occurs across the lines $L_{1,2}$ for $\Phi_{1,2}^{BO}$, respectively, where $L_1 = \{(X, Y)|X = 0, |Y| > Y_{eq}\}$ and $L_2 = \{(X, Y)|X = 0, |Y| < Y_{eq}\}$ (see red vectors in the lower panels of Fig. 1). Along these lines the sign of the p-orbital-like electronic wave functions, $\Phi_{1,2}^{BO}$, changes discontinuously. Hence, the real-valued electronic wave functions are not single valued.
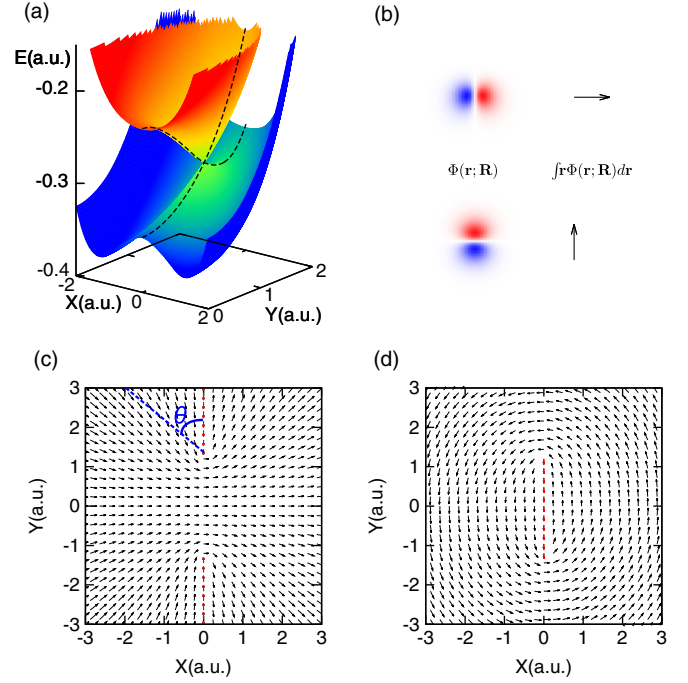

FIG. 1 (color online). (a) The first (blueish) and second (reddish) excited BO potential energy surfaces, (b) the vector field representation for p-orbital-like wave functions at a certain $\mathbf{R}$, and the BO electronic wave functions in the vector field representation for the first excited BO state (c) and the second excited BO state (d). The phase changes discontinuously across the line of red vectors (L_1 and L_2 in text).

In the exact decomposition framework, there is one potential energy surface for each exact eigenstate, $\Psi_{mol}^N(\mathbf{r}, \mathbf{R})$, of the full Hamiltonian, $\hat{H}(\mathbf{r}, \mathbf{R})$. Here, we aim at investigating the behavior of the exact potential energy surfaces in the region at and around those points where the BO surfaces show CIs. To this end, we first calculate the eigenstates of the complete system up to a certain energy, well above the CIs involving the first and second excited BO potential energy surfaces. From the computed $\Psi_{mol}^N(\mathbf{r}, \mathbf{R})$, we calculate the exact nuclear wave function in a specific gauge as $\chi_N(\mathbf{R}) = \sqrt{\int d\mathbf{r}|\Psi_{mol}^N(\mathbf{r}, \mathbf{R})|^2}$, and obtain the corresponding exact electronic wave function $\Phi_N(\mathbf{r}; \underline{\mathbf{R}}) = \Psi_{mol}^N(\mathbf{r}, \mathbf{R})/\chi_N(\mathbf{R})$. Then, for the subset of the exact electronic wave functions $\Phi_N(\mathbf{r}; \underline{\mathbf{R}})$, that exhibit p-orbital-like behavior similar to $\Phi_1^{BO}(\mathbf{r}; \mathbf{R})$ or $\Phi_2^{BO}(\mathbf{r}; \mathbf{R})$, we choose the energetically lowest two eigenstates, denoted as A and B, and calculate the exact potential energy surfaces $\epsilon_A^{ex}(\mathbf{R})$ and $\epsilon_B^{ex}(\mathbf{R})$ from Eq. (13). In Fig. 2, we have plotted $|\chi_N(\mathbf{R})|^2$, $\int \mathbf{r}\Phi_N(\mathbf{r}; \underline{\mathbf{R}})d\mathbf{r}$ and $\epsilon_N^{ex}(\mathbf{R})$ ($N = A, B$) for a nuclear mass of $M = 10.0$. The eigenenergies of $\Psi_{mol}^{A,B}$ are -0.282 and -0.201, respectively [22]. As it is seen in Fig. 2, for these exact eigenstates, $\chi_N(\mathbf{R}_{eq}^{\pm}) \neq 0$ and $\Phi_N(\mathbf{r}; \underline{\mathbf{R}})$, do not show any abrupt phase changes or singularities. Therefore, $\epsilon_A^{ex}(\mathbf{R})$ and $\epsilon_B^{ex}(\mathbf{R})$ show a smooth "diabatic" form
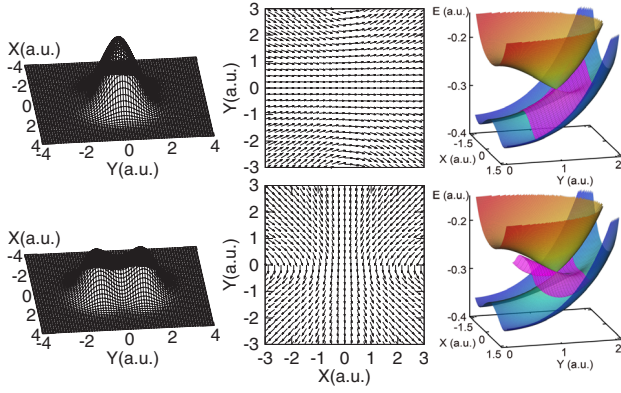
FIG. 2 (color online).   The factorized nuclear densities (left), the corresponding electronic wave functions represented by the vector fields $\int \mathbf{r}\Phi_N(\mathbf{r};\underline{\mathbf{R}})d\mathbf{r}$ (middle) and the potential energy surfaces (right) for the selected full wave functions Ψ_{mol}^A and Ψ_{mol}^B (from top to bottom) with $M = 10.0$. The blueish and reddish surfaces are the first and second excited BO potential energy surfaces, respectively, while the pink surfaces are the exact potential energy surfaces near $\mathbf{R}_{\text{eq}}^+$.

connecting ϵ_1^{BO} and ϵ_2^{BO} continuously along the Y axis through the points where, in the BO case, are CIs.

Both in the exact case and in the BO approximation the full electon-nuclear wave function $\Psi(\mathbf{r}, \mathbf{R}) = \Phi(\mathbf{r};\underline{\mathbf{R}})\chi(\mathbf{R})$ is invariant under the transformation

$$\Phi(\mathbf{r};\underline{\mathbf{R}}) \to \tilde{\Phi}(\mathbf{r};\underline{\mathbf{R}}):=e^{-iS(\underline{\mathbf{R}})}\Phi(\mathbf{r};\underline{\mathbf{R}}), \qquad (16)$$

$$\chi(\underline{\mathbf{R}}) \to \tilde{\chi}(\underline{\mathbf{R}}):=e^{iS(\underline{\mathbf{R}})}\chi(\underline{\mathbf{R}}). \qquad (17)$$

Equation (16), together with the definition of the vector potentials [Eqs. (4) and (14)], implies that the vector potential transforms as

$$\mathbf{A}_\nu(\underline{\mathbf{R}}) \to \tilde{\mathbf{A}}_\nu(\underline{\mathbf{R}}):=\mathbf{A}_\nu(\underline{\mathbf{R}}) + \nabla_\nu S(\underline{\mathbf{R}}). \qquad (18)$$

The exact equations of motion (10), (11) as well as the BO equations of motion (3), (8) are form invariant under the transformation (16)–(18). As discussed above, the real-valued electronic wave functions $\Phi_{1,2}^{\text{BO}}$ are not single valued. By performing a transformation of type (16) we can make the electronic wave function single valued and at the same time complex. To this end we choose $S(\mathbf{R}) = -\theta(\mathbf{R})/2$, where $\theta(\mathbf{R}) = \text{atan2}(X, Y - Y_{\text{eq}})$ is the angle indicated in Fig. 1(c). We then numerically calculate the geometric phase $\gamma_n^{\text{BO}}(\mathcal{L})$ from Eq. (6) using the closed path $\mathcal{L} = \{\mathbf{R}|\mathbf{R} = \mathbf{R}_{\text{eq}}^+ + R(\sin\theta, \cos\theta), 0 \leq \theta \leq 2\pi\}$ that circles around the CI at $\mathbf{R}_{\text{eq}}^+$ with the radius $R = 0.2$ a.u. The numerical integration yields $\gamma_1^{\text{BO}}(\mathcal{L}) = 3.14106$ in good agreement with π. In the exact case, the electronic wave functions $\Phi_N(\mathbf{r};\mathbf{R})$ are real *and* single valued. Hence, the vector potential (14) vanishes in the first place, and the exact Berry phase is zero.

In the following we investigate how $\Phi_A(\mathbf{r};\underline{\mathbf{R}})$, $|\chi_A(\mathbf{R})|^2$ and $\epsilon_A^{\text{ex}}(\mathbf{R})$ evolve as M increases ($M = 1, 10, 20,$ and 50) to reach the adiabatic limit ($M \to \infty$) which is

accompanied by a Berry phase. In Fig. 3, we show how the exact electronic wave function $\Phi_A(\underline{\mathbf{r}};\mathbf{R})$ transforms into Φ_1^{BO} with increasing nuclear mass. For $M = 1$, a set of vectors representing the vector field shows a mainstream simply from left to right. As M increases, however, the mainstream begins to show parabolic behavior, and the curvature of the parabola increases gradually. Compared to Φ_1^{BO} in Fig. 1, we can interpret the discontinuity along L_1 as coming from the infinite-curvature limit due to the limit $M \to \infty$. In Fig. 4, we also show $|\chi_A|^2$ and $|\epsilon_A^{\text{ex}} - \epsilon_1^{\text{BO}}|$ for various M's. As M increases, $|\chi_A|^2$ gets localized on the double-minima of ϵ_A^{ex} and also gets narrower, showing two distinctive humps. For ϵ_A^{ex}, the green region around L_1 shrinks as M increases, which means ϵ_A^{ex} gets closer to ϵ_1^{BO}, but maintaining the diabatic behavior along the Y axis. This enables us to deduce that ϵ_A^{ex} in the limit $M \to \infty$ lies on top of the BO potential energy surface ϵ_1^{BO} except for the line L_1. Since the actual nuclear mass in the real world is finite, there is no discontinuity of the electronic wave function implying that the exact geometric phase is zero.

To summarize, we have investigated whether the specific nonanalyticity in $\Phi_n^{\text{BO}}(\mathbf{r};\underline{\mathbf{R}})$ that leads to a nontrivial geometric phase in the BO approximation is a true topological feature of the full electron-nuclear wave function. To shed light on this question, we have studied a numerically exactly solvable model system in two dimensions that exhibits nontrivial Berry phases in the BO limit. Employing the exact factorization of the full molecular wave function [15–19] we identify and calculate the exact
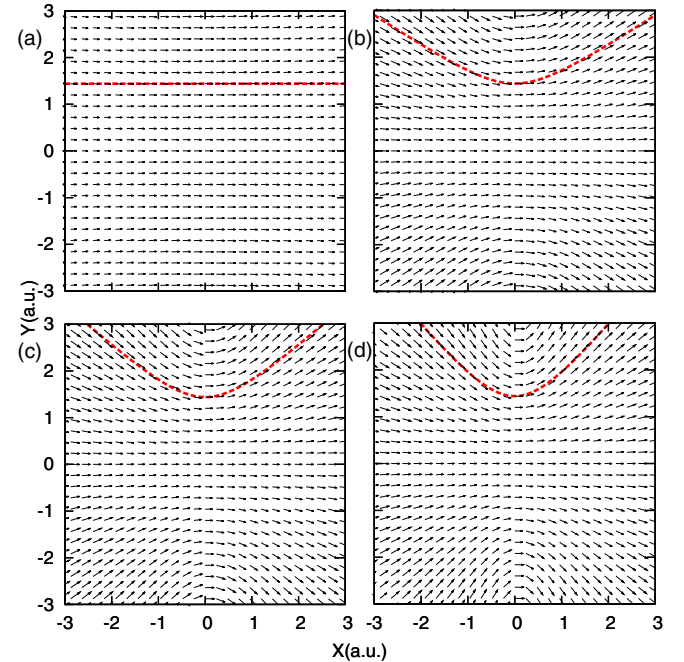

FIG. 3 (color online).   The vector $\int \mathbf{r}\Phi_A(\mathbf{r};\mathbf{R})d\mathbf{r}$ is plotted for various ionic masses, M. The values of M for the panels (a), (b), (c), and (d) are 1.0, 10.0, 20.0 and 50.0, respectively. The dashed red line indicates, as guide for the eye, the change of curvature as the ionic mass increases.
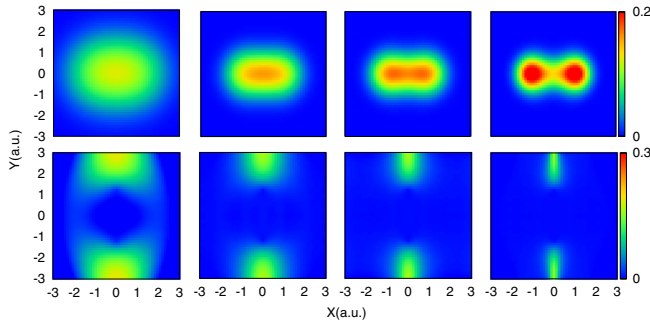
FIG. 4 (color online). The factorized nuclear densities (first row), and the difference between the exact potential energy surface and the 1st excited BO potential energy surface $(\epsilon_A^{ex} - \epsilon_1^{BO})$ (second row) for various nuclear masses ($M = 1.0$, 10.0, 20.0, and 50.0 from left to right).

electronic wave functions $\Phi_N(\mathbf{r}; \underline{\mathbf{R}})$ which, in the limit of infinite nuclear mass M, reduce to the BO electronic wave functions $\Phi_n^{BO}(\mathbf{r}; \underline{\mathbf{R}})$. We find that the exact electronic wave functions $\Phi_N(\mathbf{r}; \underline{\mathbf{R}})$ are real valued and perfectly smooth for any finite value of the nuclear mass. Consequently, the geometric phase associated with the vector potential $\mathbf{A}_{\nu,N}^{ex}(\underline{\mathbf{R}}) = -i \int \Phi_N^*(\mathbf{r}; \underline{\mathbf{R}}) \nabla_\nu \Phi_N(\mathbf{r}; \underline{\mathbf{R}}) d\mathbf{r}$ vanishes. Only in the limit $M \to \infty$ (the BO limit) a discontinuous phase change appears which leads to a nontrivial Berry phase. In this sense, the molecular Berry phase can be viewed as an artifact of the BO approximation.

We emphasize that this conclusion can be drawn only for the specific example studied here. There exist other cases [23–26] where the full problem (without invoking the adiabatic approximation) exhibits a nontrivial geometric phase. Hence, the central result of this Letter is to have demonstrated that there exist cases where a nontrivial Berry phase present in BO approximation does not have a topological counterpart in the exact electron-nuclear problem. Currently it is not known whether these cases are the majority or the exception. In [18] it was shown that the exact Berry connection (14) is closely related to the nuclear velocity field. A nonvanishing current density, both for electrons and nuclei, is encountered when the exact molecular wave function $\Psi_{mol}^N(\mathbf{r}, \underline{\mathbf{R}})$ is a complex-valued symmetry-adapted eigenfunction, e.g., of the total angular momentum operator. If the resulting velocity field has a nonvanishing curl, the vector potential (14) cannot be gauged away and hence, a nontrivial Berry phase may occur (similar to Ref. [24]). For our analysis above it is essential that the exact electronic wave function $\Phi_N(\mathbf{r}; \underline{\mathbf{R}})$ can be chosen to be real (and single valued) for all finite value of the nuclear mass M. Since, in practice, we normally cannot solve the full electron-nuclear problem, it will be extremely important to find simple mathematical criteria by which one can know (without doing the full calculation) if a nonvanishing BO-Berry phase survives in

the exact electron-nuclear treatment. This interesting—but difficult—question will be the subject of future research.

[1] L. Fu, C. L. Kane, and E. J. Mele, Phys. Rev. Lett. **98**, 106803 (2007).
[2] M. Z. Hasan and C. L. Kane, Rev. Mod. Phys. **82**, 3045 (2010).
[3] R. Resta, Rev. Mod. Phys. **66**, 899 (1994).
[4] D. Xiao, M.-C. Chang, and Q. Niu, Rev. Mod. Phys. **82**, 1959 (2010).
[5] Y. Aharonov and D. Bohm, Phys. Rev. **115**, 485 (1959).
[6] C. A. Mead, Rev. Mod. Phys. **64**, 51 (1992).
[7] D. R. Yarkony, Rev. Mod. Phys. **68**, 985 (1996).
[8] B. Kendrick, Phys. Rev. Lett. **79**, 2431 (1997).
[9] J. C. Juanes-Marcos, S. C. Althorpe, and E. Wrede, Science **309**, 1227 (2005).
[10] I. G. Ryabinkin and A. F. Izmaylov, Phys. Rev. Lett. **111**, 220406 (2013).
[11] M. V. Berry, Proc. R. Soc. A **392**, 45 (1984).
[12] C. Mead and D. Truhlar, J. Chem. Phys. **70**, 2284 (1979).
[13] F. Wilczek and A. Shapere, *Geometric Phases in Physics* (World Scientific, Singapore, 1989), Vol. 5.
[14] W. Domcke, D. Yarkony, and H. Köppel, *Conical Intersections: Electronic Structure, Dynamics & Spectroscopy* (World Scientific, Singapore, 2004), Vol. 15.
[15] N. I. Gidopoulos and E. K. U. Gross, Phil. Trans. R. Soc. A **372**, 20130059 (2014).
[16] G. Hunter, Int. J. Quantum Chem. **9**, 237 (1975).
[17] A. Abedi, N. T. Maitra, and E. K. U. Gross, Phys. Rev. Lett. **105**, 123002 (2010).
[18] A. Abedi, N. T. Maitra, and E. K. U. Gross, J. Chem. Phys. **137**, 22A530 (2012).
[19] A. Abedi, F. Agostini, Y. Suzuki, and E. K. U. Gross, Phys. Rev. Lett. **110**, 263001 (2013).
[20] S. Shin and H. Metiu, J. Chem. Phys. **102**, 9285 (1995).
[21] We use a numerical grid method with grid spacing 0.12 and 0.3 a.u. for the nuclear and electronic space, respectively. The number of grid points are 101 and 81 for each axis in nuclear and electronic space, respectively.
[22] These energies are above the energy of the CI. However, the larger the nuclear mass, the smaller the eigenenergy. For example, the eigenvalues of the state A with $M = 20.0$ and 50.0 are -0.308 and -0.329, respectively, which are well below the energy of the CI.
[23] B. Zygelman, Phys. Rev. A **86**, 042704 (2012).
[24] B. Zygelman, Phys. Rev. Lett. **64**, 256 (1990).
[25] B. Zygelman, Phys. Lett. A **125**, 476 (1987).
[26] D. Calvani, A. Cuccoli, N. I. Gidopoulos, and P. Verrucchi, Proc. Natl. Acad. Sci. U.S.A. **110**, 6748 (2013).